

*Journal of*  
***Mechanics of***  
***Materials and Structures***

**EFFECT OF ELASTIC OR SHAPE MEMORY ALLOY PARTICLES  
ON THE PROPERTIES OF FIBER-REINFORCED COMPOSITES**

Victor Birman

***Volume 4, N<sup>o</sup> 7-8***

***September 2009***

 **mathematical sciences publishers**

## EFFECT OF ELASTIC OR SHAPE MEMORY ALLOY PARTICLES ON THE PROPERTIES OF FIBER-REINFORCED COMPOSITES

VICTOR BIRMAN

The paper presents a comprehensive formulation for the analysis of the stiffness and strength of fiber-reinforced composites with the matrix enhanced by adding elastic or shape memory alloy (SMA) spheroidal particles. The micromechanical model used to evaluate the stiffness tensor of the matrix with embedded particles is based on the Benveniste version of the Mori–Tanaka theory. In the case of a superelastic shape memory alloy particulate matrix, the stiffness of the particles depends on the martensitic fraction that is in turn affected by the state of stress within the particle. In this case an exact solution for the stiffness tensor of the composite material with elastic fibers and matrix and embedded SMA particles is developed combining the recent macromechanical solution for multi-phase composites with the inverse method of the analysis of SMA. In the particular case, this solution results in explicit formulae for the homogeneous material constants of a SMA particulate material subjected to axial loading. Upon the completion of the stiffness analysis the strengths of a fiber-reinforced material with the matrix containing elastic or SMA particles can be analyzed using the Eshelby solution for the stresses. As follows from numerical examples, elastic spherical particles added to the matrix of a fiber-reinforced composite significantly improve the transverse strength and stiffness of the material, even if the volume fraction of such particles is relatively small. The effect of elastic particles on the longitudinal strength and stiffness is less pronounced. It is also illustrated that the stress-induced transformation of superelastic SMA particles results in significant changes of the properties of SMA particulate composites.

### 1. Introduction

The optimization of composite structures is usually concerned with either increasing their load-carrying capacity without additional weight or reducing weight without sacrificing the load-carrying capacity. In both situations it is necessary to enhance the stiffness and strength of the structure. The straightforward approach to achieving enhanced properties is using a stiffer high-strength material. An alternative approach employs spatially tailored structures with a variable stiffness. Functionally graded structures where the composition of the constituent phases varies in one direction only, that is, through the thickness, have also been extensively studied [Birman and Byrd 2007]. The analysis in the present paper is concerned with improving the performance of composite structures by embedding stiff high-strength elastic or SMA inclusions (particles or fibers) within the matrix of the fiber-reinforced material. The benefits of this approach for the stiffness of fibrous composite materials have recently been demonstrated by Genin and Birman [2009], who considered the effect of spherical glass particles on static and dynamic response of glass/epoxy composites.

---

*Keywords:* micromechanics, shape memory alloy composites, stiffness tensor, strength.

This study has been funded by the US Army Research Office under contract W911NF-08-1-0119 (Bruce LaMattina, Project Manager).

Embedding shape memory alloy fibers within a composite material can offer numerous advantages, including improved strength and stiffness, higher buckling loads and desirable dynamic properties. Extensive research on SMA fiber-reinforced composites with fibers that are either bonded to the substrate or embedded within resin sleeves has been reviewed in literature; see, for example, [Birman 1997]. The advantages associated with using SMA are realized through their martensitic and reverse transformations that are triggered by variations of temperature or applied stresses. In particular, the stress-induced transformation of a superelastic SMA represents an interest due to a large hysteresis loop. Accordingly, SMA materials and composites are considered for vibration control in aerospace and civil engineering applications, for example in [Lagoudas 2008; McCormick et al. 2006; Cardone et al. 2004].

The present paper illustrates a two-step micromechanical model for the stiffness and strength analysis of a fiber-reinforced material with particulate elastic or SMA matrix. The properties of the particulate matrix determined at the first step of the analysis are subsequently used to evaluate those of the fiber-reinforced material with the homogeneous matrix. As follows from numerical examples, elastic particles embedded in the matrix can significantly increase both the stiffness and the strength of fiber-reinforced materials.

In addition to the analysis of composites with elastic particulate matrices, the paper presents an exact solution for the strength and stiffness of a fiber-reinforced composite material incorporating superelastic SMA inclusions. The exact solution for the stiffness tensor is obtained by the Genin–Birman generalization of the Benveniste method combined with the three-dimensional formulation for a superelastic SMA. Contrary to available three-dimensional solutions, the present method does not involve assumptions on the law that relates the rate of change in the transformation strain to the rate of change of the martensitic fraction. Instead, the analysis of the matrix with SMA inclusions utilizes the “inverse” method. According to this method, the stresses in SMA inclusions, the applied stresses and the tensor of stiffness of the homogeneous material are determined exactly for the assumed value of the martensitic fraction. Although the inverse solution does not yield the transformation strain in SMA inclusions, this information is not necessary to determine the composite stress-strain relationships and the stiffness tensor. Once the strength and stiffness of a SMA-particulate matrix have been determined, the strength of a fiber-reinforced, SMA-particulate matrix composite can be obtained using standard solutions shown in the paper.

The analysis of SMA reinforced composites developed in the paper is applied to the case of a SMA particulate material. The explicit closed-form solution developed for this case elucidates significant variations in the stiffness of the composite as a result of applied stresses that cause SMA phase transformation.

## **2. Micromechanics of a fiber-reinforced, particulate-matrix material with elastic constituents**

Numerous methodologies of the micromechanical stiffness analysis of composites with inclusions of an arbitrary shape include the Mori–Tanaka model, the double-inclusion method, the models of Ponte Castaneda and Willis, the Kuster–Toksoz model, etc. The bounds for the stiffness tensor have been suggested by Hashin and Shtrikman, Beran, Molyneux and McCoy, Gibiansky and Torquato, etc. A comprehensive review of these techniques is outside the scope of this paper; see for example [Tucker and Liang 1999; Hu and Weng 2000; Torquato 2001; Milton 2002].

Kanaun and Jeulin [2001] and Genin and Birman [2009] proposed the solution for the stiffness tensor of a multi-phase material that is applicable to fiber-reinforced particulate composites. In particular, the latter team found that the stiffness of a cross ply glass/epoxy material evaluated using their approach was within the strict three-point bounds as long as the volume fractions of spherical inclusions and fibers remained relatively small. In the present paper the strength and stiffness analyses of a three-phase reinforced material are conducted in two steps. We begin with the Benveniste version of the Mori–Tanaka solution to specify the stiffness tensor of a particulate matrix that is subsequently applied to evaluate the stiffness of a fiber-reinforced, particulate-matrix material. The strength of the matrix with inclusions (particles) is determined using the heterogeneous matrix stiffness data. In turn, knowing the strength of the matrix enables us to predict the strength of the fiber-reinforced material with a particulate matrix. The principal reason for the two-step stiffness analysis, instead of using the solution for materials with multiple inclusion classes [Kanaun and Jeulin 2001; Genin and Birman 2009], is that the stiffness of the particulate matrix is needed for the subsequent strength analysis of the composite.

**2.1. Two-step stiffness analysis.** Consider a fiber-reinforced material where the matrix contains uniformly distributed and uniaxially aligned spheroidal inclusions (they are referred to as particles, though the approach could be applied to the case where the inclusions represent short or continuous fibers as long as we use the appropriate Eshelby tensor). It is assumed throughout the paper that the matrix is perfectly bonded to both fibers and particles. The volume fraction of the particles within the matrix remains below 30%, so that the Mori–Tanaka approach is accurate [Genin and Birman 2009]. Then the tensor of stiffness of the particulate matrix can be obtained following [Benveniste 1987] in the form

$$\mathbf{L}_{\text{pm}} = \mathbf{L}_1 + f'_2(\mathbf{L}_2 - \mathbf{L}_1)\mathbf{T}_2(f'_1\mathbf{I} + f'_2\mathbf{T}_2)^{-1}, \quad (1)$$

where the subscripts 1 and 2 identify the matrix and particles, respectively,  $\mathbf{L}_i$  is the stiffness tensor of the corresponding phase,  $\mathbf{I}$  is the fourth-order identity tensor,  $f'_i$  is the volume fraction of the  $i$ -th phase, and the prime indicates that these volume fractions are evaluated within the particulate matrix, that is,  $f'_1 + f'_2 = 1$ . Furthermore,

$$\mathbf{T}_2 = [\mathbf{I} + \mathbf{S}_2\mathbf{L}_1^{-1}(\mathbf{L}_2 - \mathbf{L}_1)]^{-1} \quad (2)$$

is the coefficient tensor in the relation between the strain tensors in the matrix and in the particles

$$\boldsymbol{\varepsilon}_2 = \mathbf{T}_2\boldsymbol{\varepsilon}_1. \quad (3)$$

The elements of the Eshelby tensor  $\mathbf{S}_2$  were obtained for spheroidal inclusions dependent on the aspect ratio by Tandon and Weng [1986].

It is known that the Mori–Tanaka solution for the bulk, elasticity and shear moduli of particulate composites coincides with the Hashin–Shtrikman lower bound. At a high volume fraction of particles the Mori–Tanaka prediction deviates from numerical (FEA) and experimental results. However, the accuracy of the analysis at high particle volume fractions can be improved using the incremental particle-addition approach suggested in the Appendix.

Once the stiffness tensor of the particulate matrix has been evaluated, it is possible to treat the matrix as a homogeneous medium that is isotropic if the particles are isotropic and spherical or if they are randomly oriented. Subsequently, we can apply a similar homogenization procedure to a unidirectional

fiber-reinforced material considering fibers as aligned inclusions with an infinite aspect ratio. Accordingly, the stiffness tensor of such fiber-reinforced, particulate-matrix material is

$$\mathbf{L} = \mathbf{L}_{\text{pm}} + f_3(\mathbf{L}_3 - \mathbf{L}_{\text{pm}})\mathbf{T}_3(f_{\text{pm}}\mathbf{I} + f_3\mathbf{T}_3)^{-1}, \quad (4)$$

where  $f_3$  and  $f_{\text{pm}}$  are the volume fractions of fibers and particulate matrix, respectively,  $f_{\text{pm}} + f_3 = 1$ , and

$$\mathbf{T}_3 = [\mathbf{I} + \mathbf{S}_3\mathbf{L}_{\text{pm}}^{-1}(\mathbf{L}_3 - \mathbf{L}_{\text{pm}})]^{-1} \quad (5)$$

The Eshelby tensor for a fiber-reinforced material with an isotropic homogenous matrix,  $\mathbf{S}_3$ , was obtained by [Luo and Weng \[1989\]](#). Alternative micromechanical methods that could be applied to the analysis of a fiber-reinforced material with the isotropic particulate matrix properties determined as shown above include the well-known Halpin–Tsai or mechanics of materials solutions.

**2.2. Strength of a particulate matrix.** The pioneering study of [Eshelby \[1957\]](#) provided expressions for the stresses just outside a spheroidal inclusion. This work was further continued by [Tandon and Weng \[1986\]](#) and [Kakavas and Kontoni \[2005\]](#) who also illustrated that the analytical results were in a good agreement with the finite element analysis.

Micromechanical strength conditions can be determined by specifying the stress in the matrix, at the particle-matrix interface, and in the particles, and subsequently applying strength criteria to the matrix and particles and at the interface. In this paper, we assume a perfect bond between the matrix and particles. Furthermore, the fracture analysis is not included, though it could be developed based on the knowledge of local stresses and assuming that the crack originates at the particle-matrix interface. The strength of the particles is assumed higher than that of the matrix (as is usually the case in applications), so that failure initiates in the matrix, just outside the particles, where the stresses are elevated due to the stress concentration. Among the strength criteria applicable to the analysis of the isotropic and ductile matrix, we consider the maximum principal stress criterion and the von Mises criterion. In the case of a brittle matrix, these criteria may be inaccurate and the Coulomb–Mohr criterion or the recently suggested Christensen criterion [\[2007\]](#) becomes more appropriate.

Consider a particulate matrix subject to uniaxial tension  $\hat{\sigma}_{11}$  (the in-plane coordinates referred to are denoted by 1 and 2). The stresses in the matrix (in the 1-2 plane), just outside a spherical particle, are [\[Tandon and Weng 1986\]](#)

$$\begin{aligned} \sigma_{11,m} &= \hat{\sigma}_{11} \left( 1 + \frac{(1-f'_2)(b_1p_1 + 2b_2p_2)}{(1+\nu_1)(1-2\nu_1)} + \frac{p_1 \cos^2 \theta + p_2(\nu_1 + \sin^2 \theta)}{1-\nu_1^2} \cos^2 \theta \right) = F_{11}(\theta)\hat{\sigma}_{11} \\ \sigma_{22,m} &= \hat{\sigma}_{11} \left( \frac{(1-f'_2)(b_3p_1 + (b_4 + b_5)p_2)}{(1+\nu_1)(1-2\nu_1)} + \frac{p_1 \cos^2 \theta + p_2(\nu_1 + \sin^2 \theta)}{1-\nu_1^2} \sin^2 \theta \right) = F_{22}(\theta)\hat{\sigma}_{11} \\ \sigma_{33,m} &= \hat{\sigma}_{11} \left( \frac{(1-f'_2)(b_3p_1 + (b_4 + b_5)p_2)}{(1+\nu_1)(1-2\nu_1)} + \frac{\nu_1 p_1 \cos^2 \theta + p_2(1 + \nu_1 \sin^2 \theta)}{1-\nu_1^2} \right) = F_{33}(\theta)\hat{\sigma}_{11} \\ \sigma_{12,m} &= -\hat{\sigma}_{11} \frac{p_1 \cos^2 \theta + p_2(\nu_1 + \sin^2 \theta)}{1-\nu_1^2} \sin \theta \cos \theta = F_{12}(\theta)\hat{\sigma}_{11} \\ \sigma_{13,m} &= \sigma_{23,m} = 0, \end{aligned} \quad (6)$$

where the coefficients  $b_j$  and  $p_j$  are specified according to [Tandon and Weng 1986] in terms of the elements of Eshelby's tensor, the particle volume fraction within the particulate matrix  $f'_2$ , and bulk and shear moduli of the matrix and particles.

The principal stresses can now be determined from

$$\begin{vmatrix} \sigma_{11,m} - \sigma & \sigma_{12,m} & 0 \\ \sigma_{12,m} & \sigma_{22,m} - \sigma & 0 \\ 0 & 0 & \sigma_{33,m} - \sigma \end{vmatrix} = 0. \quad (7)$$

Accordingly,

$$\begin{aligned} \sigma_{1,2} &= \hat{\sigma}_{11} \left( \frac{F_{11}(\theta) + F_{22}(\theta)}{2} \pm \sqrt{(F_{11}(\theta) - F_{22}(\theta))^2 + 4F_{12}^2(\theta)} \right) = \hat{\sigma}_{11} F_{1,2}(\theta), \\ \sigma_3 &= \hat{\sigma}_{11} F_{33}(\theta). \end{aligned} \quad (8)$$

The maximum principal stress criterion yields the tensile strength of the particulate matrix:

$$s_{pm,T} = s_{mT} \min\{F_1^{-1}(\theta), F_2^{-1}(\theta), F_{33}^{-1}(\theta)\}, \quad (9)$$

where  $s_{mT}$  is the tensile strength of the matrix material.

The von Mises strength criterion predicts the strength

$$s_{pm,T} = \sqrt{2} s_{mT} ([F_1(\theta) - F_2(\theta)]^2 + [F_1(\theta) - F_{33}(\theta)]^2 + [F_2(\theta) - F_{33}(\theta)]^2)^{-1/2}. \quad (10)$$

Either one uses the strength criterion (9) or (10), it is necessary to check all values of  $0 \leq \theta \leq \pi/2$  since it is unpractical to analytically determine the angular coordinate corresponding to the onset of failure. Therefore, the strength should be found as the smallest value of the stress given by (9) or (10) obtained by varying the angular coordinate.

The analysis of the axial compressive strength is quite similar: we can use (9) or (10), where  $s_{pm,T}$  is replaced with the compressive strength of the particulate matrix  $s_{pm,C}$  and  $s_{mT}$  is replaced with the compressive strength of the matrix material  $s_{mC}$ .

Now consider the shear strength of the particulate matrix subject to the stress  $\hat{\sigma}_{12}$ . Let

$$R = (1 - f'_2)(1 - 2S_{1212}) - \frac{G_2}{G_2 - G_1} \quad \text{and} \quad S = \frac{(1 - f'_2)(1 - 2S_{1212}) \left(1 - \frac{2G_1}{G_{pm}}\right) - \frac{G_2}{G_2 - G_1}}{(1 - f'_2)(1 - 2S_{1212}) - \frac{G_2}{G_2 - G_1}}, \quad (11)$$

where  $G_1$  and  $G_2$  are the shear moduli of the matrix and particles, respectively, and  $G_{pm}$  is the shear modulus of the particulate matrix found using the solution in the previous section. Then the stresses in the matrix adjacent to the particle can be obtained [Tandon and Weng 1986]:

$$\begin{aligned} \sigma_{11,m} &= -\frac{4G_1}{(1 - \nu_1)G_{pm}R} \hat{\sigma}_{12} \sin \theta \cos^3 \theta = \tilde{F}_{11}(\theta) \hat{\sigma}_{12}, \\ \sigma_{22,m} &= -\frac{4G_1}{(1 - \nu_1)G_{pm}R} \hat{\sigma}_{12} \sin^3 \theta \cos \theta = \tilde{F}_{22}(\theta) \hat{\sigma}_{12}, \end{aligned} \quad (12)$$

$$\begin{aligned} \sigma_{33,m} &= -\frac{4G_1\nu_1}{(1-\nu_1)G_{pm}R}\hat{\sigma}_{12}\sin\theta\cos\theta = \tilde{F}_{33}(\theta)\hat{\sigma}_{12}, \\ \sigma_{12,m} &= \hat{\sigma}_{12}\left(S + \frac{4G_1}{(1-\nu_1)G_{pm}R}\sin^2\theta\cos^2\theta\right) = \tilde{F}_{12}(\theta)\hat{\sigma}_{12}, \\ \sigma_{13,m} &= \sigma_{23,m} = 0. \end{aligned}$$

These expressions depend on the shear modulus of the particulate matrix, which is available from the micromechanical solution.

The principal stresses found from (7) are

$$\begin{aligned} \sigma_{1,2} &= \hat{\sigma}_{12}\left(\frac{\tilde{F}_{11}(\theta) + \tilde{F}_{22}(\theta)}{2} \pm \sqrt{(\tilde{F}_{11}(\theta) - \tilde{F}_{22}(\theta))^2 + 4\tilde{F}_{12}^2(\theta)}\right) = \hat{\sigma}_{12}\tilde{F}_{1,2}(\theta), \\ \sigma_3 &= \hat{\sigma}_{12}\tilde{F}_{33}(\theta). \end{aligned} \tag{13}$$

Subsequently, the maximum principal stress criterion or the von Mises criterion yields the shear strength of the particulate matrix in the form (9) and (10), respectively, where  $F_1$  is replaced by  $\tilde{F}_1$ ,  $F_2$  by  $\tilde{F}_2$ ,  $F_{33}$  by  $\tilde{F}_{33}$ ,  $s_{pm,T}$  by  $s_{pm,S}$  (the particulate matrix shear strength) and  $s_{mT}$  by the matrix shear strength  $s_{mS}$ . Similarly to the case for the tensile and compressive strengths, the shear strength of the particulate matrix is found as the smallest stress obtained from the accordingly modified equations (9) or (10) by varying the values of  $\theta$ .

**2.3. Strength of the fiber-reinforced material with a homogenized matrix.** The outline of micromechanical solutions for the strengths of a fiber-reinforced material in the axial and transverse directions as well as for the shear strength obtained by assumption that all constituents remain within the linear elastic range and bonding between the fibers and matrix is not violated was given by Daniel and Ishai [2006]. These solutions are outlined here using the properties of fibers and those of the particulate matrix, for completeness. The composite strengths depend on the strength of fibers that we assume known and on the strength, ultimate strain and stiffness of the particulate matrix evaluated using the results shown in the previous sections.

The longitudinal tensile strength  $s_{1T}$  depends on the relationship between the ultimate longitudinal tensile strain  $\epsilon_{f,l}^u$  of the fibers and the ultimate tensile strain  $\epsilon_{pm}^u = s_{pm,T}/E_{pm}$  of the particulate matrix (here  $E_{pm}$  is the elastic modulus of the particulate matrix):

$$\begin{aligned} s_{1T} &= s_{fT}\left(f_3 + f_{pm}\frac{E_{pm}}{E_3}\right) \quad \text{if } \epsilon_{f,l}^u < \epsilon_{pm}^u, \\ s_{1T} &= s_{pm,T}\left(f_3\frac{E_3}{E_{pm}} + f_{pm}\right) \quad \text{if } \epsilon_{f,l}^u > \epsilon_{pm}^u, \end{aligned} \tag{14}$$

where  $s_{fT}$  is the tensile strength of isotropic fibers and  $E_3$  is their modulus of elasticity.

The modes of failure of a unidirectional fiber-reinforced composite subject to longitudinal compression include fiber microbuckling in either extensional or shear mode and shear failure. The microbuckling

failure modes occur at the following value of the applied compressive stress

$$s'_{1C} = \min \left\{ 2f_3 \sqrt{\frac{E_{pm} E_3 f_3}{3 f_{pm}}}, \frac{G_{pm}}{f_{pm}} \right\}, \quad (15)$$

where  $G_{pm}$  is the shear modulus of the particulate matrix.

The shear failure mode of a longitudinally compressed fiber-reinforced material occurs at the stress

$$s''_{1C} = 2s_{fs} \left( f_3 + f_{pm} \frac{E_{pm}}{E_3} \right), \quad (16)$$

where  $s_{fs}$  is the shear strength of the fiber.

The longitudinal compressive strength is now found as  $s_{1C} = \min\{s'_{1C}, s''_{1C}\}$ . The analysis can also account for the effect of fiber misalignment, as discussed by [Daniel and Ishai \[2006\]](#).

The transverse tensile failure of fiber-reinforced composites can be predicted accounting for the stress or strain concentration factor and for residual stresses. For example, the stress concentration factor for a square array of fibers can be obtained in terms of the properties of the particulate matrix and fibers as

$$k = \frac{1 - f_3(1 - E_{pm}/E_3)}{1 - \sqrt{4f_3/\pi}(1 - E_{pm}/E_3)}. \quad (17)$$

Subsequently, the maximum principal stress criterion yields  $s_{2T} = (s_{pmT} - \sigma_{pm,res})/k$ , where  $\sigma_{pm,res}$  is the maximum radial residual stress in the particulate matrix. The latter stress can be found using a concentric cylinder model subject to a uniform temperature, the inner cylinder being the fiber, surrounded with a cylindrical layer of the particulate matrix that is in turn surrounded with the fiber-reinforced medium. A more accurate approach would be based on subdividing the cylindrical layer of the particulate matrix into a thin cylinder of the matrix material encompassed with a cylinder of the particulate matrix material. The radial coordinate of the interface between these two cylinders could be determined from geometric considerations. An alternative formulation employing the maximum principal strain criterion is also available using the properties of the particulate matrix and the maximum residual radial strain.

The compressive strength of a fiber-reinforced composite is the lesser failure stress corresponding to a number of possible scenarios, including interfacial shear failure, debonding and fiber crushing. The typical mode of failure being the compressive matrix failure, the strength is determined as  $s_{2C} = (s_{pm,C} + \sigma_{pm,res})/k$ .

In-plane shear failure occurs as a result of the interfacial shear stress concentration. The stress concentration factor  $k_{sh}$  is available from (17) by replacing the moduli of elasticity with the shear moduli of the corresponding phases. Then the shear strength is  $s_{12} = s_{pm,S}/k_{sh}$ .

The strengths of the fiber-reinforced material can be specified only upon the conclusion of the micro-mechanical stiffness analysis presented above, since they depend on the stiffness of the particulate matrix.

### 3. Fiber-reinforced composite material with superelastic shape memory alloy inclusions embedded within the matrix

The total strain in SMA is composed of elastic, transformation and thermal components. The latter components are negligible in the material experiencing superelastic transformations. The increments of the transformation strain are usually evaluated as functions of the increments of the martensitic volume

fraction using an assumption regarding the incremental law; see for example, [Boyd and Lagoudas 1993; Birman et al. 1996; Jonnalagadda et al. 1998; Jiang and Batra 2002]. An alternative theory [Lu and Weng 2000] treated the martensitic phase as a separate class of inclusions within the austenitic metal.

Contrary to the incremental approach referred to above, the present solution is exact, yielding the stiffness and applied stress and strain tensors for a material with superelastic SMA inclusions (spheroidal particles or fibers) corresponding to a prescribed martensitic fraction of SMA (other types of inclusions, besides SMA, can also be present).

The solution follows this sequence:

- (i) The Benveniste version of the Mori–Tanaka formulation for a composite material with multiple classes of inclusions is outlined, following the solution by Genin and Birman [2009].
- (ii) A three-dimensional formulation for the superelastic material is then presented, combining the approaches of [Boyd and Lagoudas 1993] and [Tanaka 1986; Sato and Tanaka 1988].
- (iii) A combination of the micromechanical and superelastic SMA formulations above, together with the inverse method suggested in this paper, is used to obtain the exact solution for the stress-strain response and stiffness of a composite material with multiple inclusions, including superelastic SMA particles or fibers.

The analysis is practical since the knowledge of the transformation strain is not needed in numerous problems concerned with SMA composites. Using the present solution that provides the applied stresses, stiffness and stress-strain relationships corresponding to a prescribed martensitic volume fraction in SMA inclusions, one can also develop a complete hysteresis loop varying this volume fraction to predict the damping capacity of superelastic SMA composites bypassing the evaluation of the transformation strain (this study elucidating a remarkable damping potential of particulate SMA composites is the subject of a separate paper).

**3.1. Micromechanics of a composite material with numerous inclusion classes.** Consider a representative volume element of a composite material with multiple inclusions of various shapes and properties subject to a remote strain tensor  $\bar{\epsilon}_0$ . The behavior of SMA undergoing martensitic or reverse transformation is physically nonlinear. However, if the martensitic fraction of SMA is known, we can employ a tangent stiffness tensor of the corresponding inclusions. All inclusions are assumed perfectly bonded to the matrix. The average stress tensor in the element is related to the tensor of the applied average strain via the tangent stiffness tensor by

$$d\sigma_0 = L d\epsilon_0. \quad (18)$$

Following the solution by Genin and Birman [2009], the stiffness tensor is expressed in terms of the corresponding tensors of the matrix ( $i = 1$ ) and inclusions ( $i > 1$ ) by the following equation, which represents an extrapolation of (1):

$$\mathbf{L} = \mathbf{L}_1 + \sum_{i=2}^N f_i (\mathbf{L}_i - \mathbf{L}_1) \mathbf{T}_i (f_1 \mathbf{I} + f_2 \mathbf{T}_2 + \cdots + f_N \mathbf{T}_N)^{-1}, \quad (19)$$

where the number of distinct inclusion classes is  $N-1$  and the  $f_i$  are the volume fractions of the matrix ( $i = 1$ ) and inclusions ( $i \geq 2$ ). In the following discussion, SMA inclusions are identified by  $i = 2$ .

Tensors  $T_i$  are given by equations similar to (2). Note that the Eshelby tensor  $S_2$  for SMA inclusions is not affected by the martensitic transformation as long as the stiffness of the matrix remains constant [Boyd and Lagoudas 1993].

In the following solution, we employ relationships between the tensor of average applied strain and the tensor of average strain within the inclusions

$$d\boldsymbol{\varepsilon}_i = \mathbf{A}_i(\xi) d\boldsymbol{\varepsilon}_0, \quad (20)$$

where the so-called tensors of concentration factors are given by

$$\mathbf{A}_i = \mathbf{T}_i(f_1\mathbf{I} + f_2\mathbf{T}_2 + \cdots + f_N\mathbf{T}_N)^{-1}. \quad (21)$$

Note that the Genin–Birman solution (19) differs from that using a two-step approach, that is, Equations (1) and (4). A quantitative comparison of the accuracy of these two approaches is outside our scope here.

**3.2. Three-dimensional formulation for a shape memory material.** The following formulation employs the assumption that the tensor of stiffness of a SMA material during the martensitic or reverse transformation can be represented by the rule of mixtures [Boyd and Lagoudas 1993]

$$\mathbf{L}_2 = \mathbf{L}_2^A + \xi(\mathbf{L}_2^M - \mathbf{L}_2^A), \quad (22)$$

where the superscripts  $A$  and  $M$  refer to the austenitic and martensitic phase of the material.

Note that the rule of mixtures can also be applied to the strength of the SMA material, so that

$$s_2 = s_2^A + \xi(s_2^M - s_2^A). \quad (23)$$

The three-dimensional constitutive relations for a superelastic shape memory material are

$$d\boldsymbol{\sigma}_2 = d(\mathbf{L}_2(\boldsymbol{\varepsilon}'_2 - \boldsymbol{\varepsilon}^t_2)), \quad (24)$$

where  $\boldsymbol{\varepsilon}'_2$  and  $\boldsymbol{\varepsilon}^t_2$  are tensors of total and transformation strains, respectively. The rate of change of the tensor  $\boldsymbol{\varepsilon}^t_2$  is related to the rate of change of the martensitic volume fraction, using an assumption for the tensor of coefficients in the relationship (called the *transformation tensor*). This approach implies the use of an incremental technique monitoring the changes in the tensors of strain and stress with the changes in the martensitic volume fraction; see, for example, [Birman et al. 1996; Jonnalagadda et al. 1998; Jiang and Batra 2002].

In the present study we discard the assumption regarding the transformation tensor and operate with the average elastic strain tensor within the SMA particle, that is,  $\boldsymbol{\varepsilon}_2 = \boldsymbol{\varepsilon}'_2 - \boldsymbol{\varepsilon}^t_2$ . This enables us to directly apply linear elastic micromechanical theories, such as the Mori–Tanaka theory and its extrapolation to multi-phase composites outlined in the previous section. While the present approach does not provide tools for a decomposition of the elastic strain and determining the transformation component, it is sufficient in a number of applied problems.

Equation (24) can be replaced with the following incremental relationship utilizing the tangent SMA stiffness tensor:

$$d\boldsymbol{\sigma}_2 = \mathbf{L}_2(\xi) d\boldsymbol{\varepsilon}_2. \quad (25)$$

The martensitic fraction can be related to the effective stress in SMA by extrapolating the solutions for a number of available one-dimensional theories (such as Tanaka's, Liang–Rogers' and Brinson's

theories). As an example, we adopt the Tanaka model [Tanaka 1986; Sato and Tanaka 1988]:

$$\begin{aligned}\zeta &= 1 - \exp[b_M(T_S^M - T) + c_M\sigma_{\text{eff}}] & (A \rightarrow M), \\ \zeta &= \exp[b_A(T_S^A - T) + c_A\sigma_{\text{eff}}] & (M \rightarrow A),\end{aligned}\quad (26)$$

where  $T$  is the current temperature,  $T_S^M$  and  $T_S^A$  are the martensite and austenite phase start temperatures at stress-free conditions, and  $b_M$ ,  $b_A$ ,  $c_M$ ,  $c_A$  are constants [Birman et al. 1996].

The effective stress is defined in terms of the components of the deviatoric stress tensor, that is,

$$\sigma_{\text{eff}} = \sqrt{\frac{3}{2}\sigma'_{ij}\sigma'_{ij}}, \quad \sigma'_{ij} = \sigma_{ij} - \frac{1}{3}\sigma_{nn}\delta_{ij}, \quad (27)$$

where  $\sigma_{ij} = \sigma_0^{(ij)}$ .

**3.3. Stiffness of a composite material with SMA particles: exact inverse method.** For a composite material where several inclusion classes, including superelastic particles, are embedded within an elastic matrix, we now develop an exact solution to relate the tensor of applied strain to the martensitic fraction in SMA particles and to determine the stiffness tensor corresponding to this applied strain.

Consider the situation where the tensor of applied strain  $\boldsymbol{\varepsilon}_0$  is prescribed, except for one component  $\varepsilon_0^{(mn)}$  that will be specified from the subsequent solution. We begin by assuming the average martensitic volume fraction  $\zeta$  in SMA particles (the average per the inclusion class approach to strains and stresses adopted in the Mori–Tanaka micromechanics necessitates the use of the average martensitic volume fraction). The corresponding value of the effective stress  $\sigma_{\text{eff}}$  in the particle is immediately available from (26), dependent on the transformation being direct or reversed (temperature is assumed constant). Subsequently, the SMA stiffness tensor  $\mathbf{L}_2$  corresponding to  $\zeta$  can be determined from (22), and the composite stiffness tensor  $\mathbf{L}$  is specified from (19). While these tensors are the ultimate goal of the analysis, the solution cannot stop here since we need to specify the unknown component of the applied strain tensor corresponding to the assumed martensitic volume fraction.

The tensors  $\mathbf{T}_i$  for each class of inclusions can be determined from equations similar to (2), where the Eshelby tensor is not affected by the transformation within SMA particles. Subsequently, (21) yields the concentration tensors  $\mathbf{A}_i$ .

We have a system of 13 equations obtained from (23), (20) and (27) with respect to twelve unknown components of the SMA stress and strain tensor increments, and the component of applied strain increment  $d\varepsilon_0^{(mn)}$ . The solution is incremental, starting with the elastic case where SMA particles are in the austenitic phase (in this case the solution is available using [Tandon and Weng 1986]). At each subsequent increment of the martensitic fraction the corresponding effective stress is found from (26). The SMA and composite material tangent stiffness tensors are specified from (22) and (19). Subsequently, equations (20) are used to express all strain components in the SMA inclusions, i.e.,  $\boldsymbol{\varepsilon}_2 = \boldsymbol{\varepsilon}_2(\varepsilon_0^{(mn)}, \zeta)$ . The final phase of the solution is finding the values of  $\varepsilon_0^{(mn)}$  and six components of the stress tensor in SMA inclusions from (25) and (27).

The strength of SMA particles corresponding to the prescribed martensitic volume fraction is available from (23). Using the strength and stiffness of the SMA particles corresponding to the applied strain tensor, the strength analysis of a fiber-reinforced, SMA particulate matrix composite can be conducted using the previously illustrated solution.

**3.4. Particular case: superelastic SMA particulate composite material.** As an example illustrating an application of the inverse method of analysis discussed in the previous section consider the case of an isotropic matrix with spherical SMA particles subject to a uniaxial axial stress  $\hat{\sigma}_0^{(11)}$ . As shown in [Tandon and Weng 1986], the stresses in a particle subject to a uniaxial loading are

$$\begin{aligned} d\sigma_2^{(11)} &= \left(1 + \frac{1 - f_2'}{(1 + \nu_1)(1 - 2\nu_1)}(b_1 p_1 + 2b_2 p_2)\right) d\hat{\sigma}_0^{(11)}, \\ d\sigma_2^{(22)} &= d\sigma_2^{(33)} = \frac{1 - f_2'}{(1 + \nu_1)(1 - 2\nu_1)}(b_3 p_1 + (b_4 + b_5)p_2) d\hat{\sigma}_0^{(11)}, \\ d\sigma_2^{(mn)} &= 0, \quad m \neq n, \end{aligned} \quad (28)$$

where  $b_j$  and  $p_j$  are coefficients specified in that reference. These coefficients depend on the stiffness of SMA particles, that is,  $b_j = b_j(\zeta)$  and  $p_j = p_j(\zeta)$ .

The increment of the effective stress in SMA particles can now be explicitly expressed in terms of the increment of the applied stress

$$d\sigma_{\text{eff}} = |d\sigma_2^{(11)} - d\sigma_2^{(22)}| = \left|1 + \frac{1 - f_2'}{(1 + \nu_1)(1 - 2\nu_1)}((b_1 - b_3)p_1 + (2b_2 - b_4 - b_5)p_2)\right| d\hat{\sigma}_0^{(11)}. \quad (29)$$

Explicit expressions for the shear and bulk moduli of a composite material consisting of the matrix with embedded spherical particles, that is,  $G_{\text{pm}}$  and  $K_{\text{pm}}$ , are available [Vel and Batra 2004]

$$G_{\text{pm}} = G_1 + \frac{f_2'(G_2 - G_1)}{1 + f_1' \frac{G_2 - G_1}{G_1 + \rho}}, \quad K_{\text{pm}} = K_1 + \frac{f_2'(K_2 - K_1)}{1 + f_1' \frac{G_2 - G_1}{K_1 + 4G_1/3}}, \quad \rho = \frac{G_1(9K_1 + 8G_1)}{6(K_1 + 2G_1)}. \quad (30)$$

The elasticity modulus and the Poisson ratio of the SMA-particulate material can now be determined from  $E_{\text{pm}} = 9K_{\text{pm}}G_{\text{pm}}(3K_{\text{pm}} + G_{\text{pm}})^{-1}$  and  $\nu_{\text{pm}} = E_{\text{pm}}(2G_{\text{pm}})^{-1} - 1$ .

The computational procedure in this case is very simple. The initial step corresponds to the elastic problem with austenitic SMA particles where the solution is available. Then the martensitic fraction is increased incrementally. At each value of  $\zeta$  one can find the corresponding stiffness characteristics of SMA particles and composite material from (22) and (19), while the effective stress is specified from (26). The coefficients  $b_j = b_j(\zeta)$  and  $p_j = p_j(\zeta)$  are also calculated at this step. Subsequently, (29) yields the value of the applied stress, while (30) results in the stiffness of the particulate material corresponding to this stress. The strain tensor in the composite material is determined using (18).

#### 4. Numerical examples

The effectiveness of embedding stiff particles within the matrix of a fiber-reinforced composite is shown on the example of a glass/epoxy material with spherical particles within the matrix. The properties of the constituent materials are taken as in [Genin and Birman 2009]:  $E_1 = 3.12$  GPa,  $\nu_1 = 0.38$ ,  $E_2 = E_3 = 76.0$  GPa,  $\nu_2 = \nu_3 = 0.25$ . The tensile stress ratio  $k_{\text{pm}} = \sigma_{11,m}(\text{max})/\hat{\sigma}_{11}$  as a result of uniaxial tension is shown in Figure 1, left, where the maximum stress in the matrix is normalized with respect to the stress applied to the particulate matrix. The case of  $f_2' = 0$  corresponds to a single particle embedded within the matrix, while larger values of the particle volume fraction account for multiple inclusions.

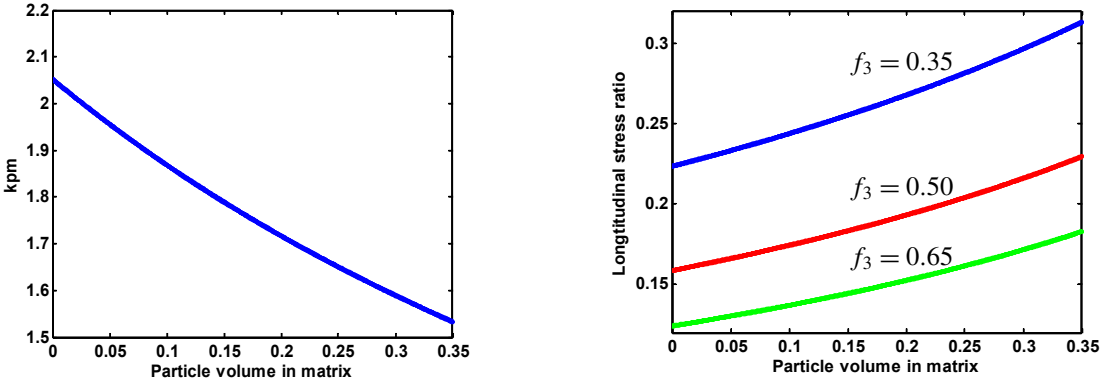


**Figure 1.** Tensile stress ratio ( $k_{pm}$ ) in (left) the particulate matrix subject to uniaxial tension, and (right) fiber-reinforced particulate-matrix composite.

The stress ratio reaches a maximum in the case of a single particle as was also observed by Tandon and Weng [1986]. In Figure 1, right, we see the tensile stress concentration ratio at the composite level, that is, the ratio  $\sigma_{11,m}(\max)/\sigma_{11}^0$  of the maximum stress in the matrix to the applied composite stress.

The beneficial effect of adding particles on the longitudinal and transverse stiffness of the fiber-reinforced material is reflected in Figure 2. The longitudinal stiffness of the material with a homogeneous

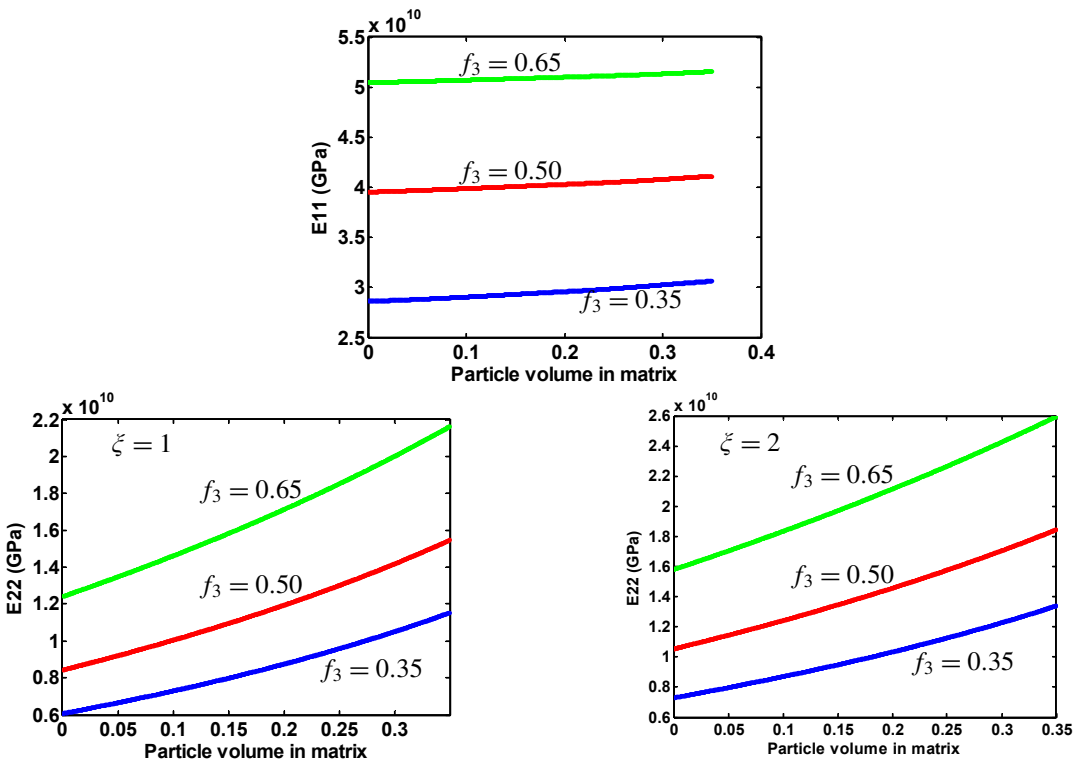


**Figure 2.** Effect of particle volume fraction in particulate matrix on longitudinal (top) and transverse (bottom) stiffness of fiber-reinforced composite.

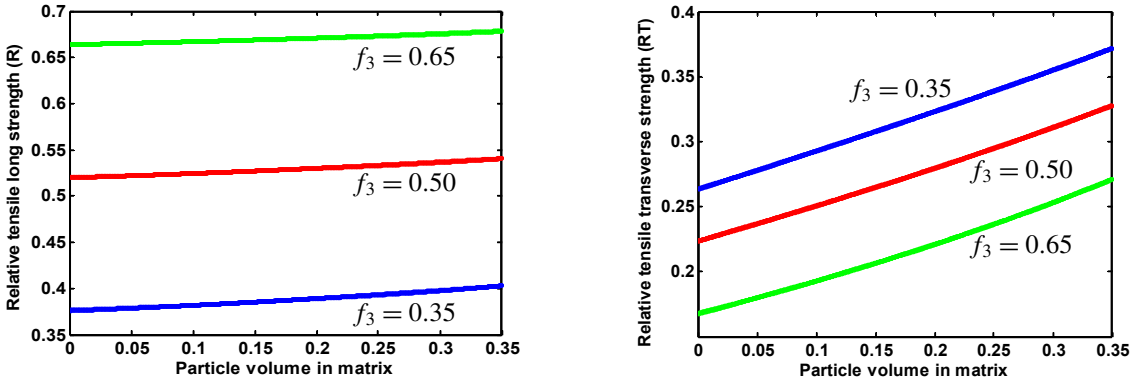


**Figure 3.** Effect of particles on the tensile longitudinal (left) and transversal (right) strength of fiber-reinforced particulate-matrix composite. ( $R = s_{1T}/s_{fT}$ )

particulate matrix was determined by the rule of mixtures. The transverse stiffness was determined by the Halpin–Tsai model with the curve fitting parameter equal to  $\zeta = 1$  and  $\zeta = 2$  (typical range of this parameter). As seen in Figure 2, even a modest amount of particles added to the matrix can significantly enhance the transverse stiffness, although the effect on the longitudinal stiffness is less pronounced.

The effect of particles on the longitudinal tensile strength of the composite material is reflected in Figure 3, left, for the case where  $\varepsilon_{f,l}^u < \varepsilon_{pm}^u$ . As is obvious from that figure, adding glass particles to the matrix has a relatively small effect on the longitudinal strength of the material. Predictably, the situation is different in the case of transverse strength since it is highly dependent on the strength of the particulate matrix. As is shown in Figure 3, right, the effect of adding particles on the transverse strength of the composite is much more pronounced than that on its longitudinal strength. This is expected since the contribution of the matrix to the transverse strength is higher than that to the longitudinal strength.

Examples of the closed-form solution for composites including SMA Nitinol spherical particles embedded within an epoxy matrix with the properties identical to those in the paper on fibrous SMA composites by Birman et al. [1996] are presented below. Figure 4 shows the shear and elasticity moduli as functions

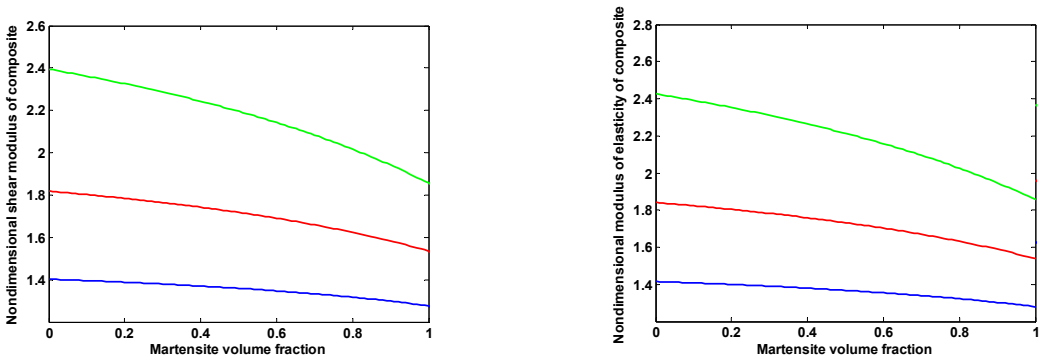


**Figure 4.** Shear modulus and elasticity modulus of SMA particulate composite (relative to those of epoxy), as functions of the martensitic fraction. The SMA volume fraction is  $f_2 = 0.20$  (blue),  $f_2 = 0.35$  (red), and  $f_2 = 0.50$  (green).

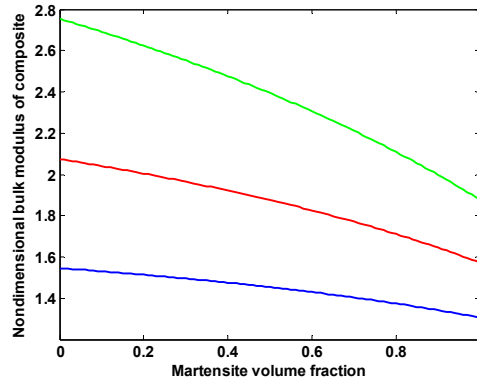


**Figure 5.** Bulk modulus of SMA particulate composite (relative to that of epoxy), as a function of the martensitic fraction. The SMA volume fraction is  $f_2 = 0.20$  (blue),  $f_2 = 0.35$  (red), and  $f_2 = 0.50$  (green).

of the martensitic volume fraction, for values of the SMA particle volume fraction equal to 20%, 35%, and 50%, while Figure 5 does the same for the bulk modulus. As is evident from these figures, martensitic and reverse phase transformations in SMA particles significantly affect the properties of SMA particulate composites with a high SMA volume fraction. The changes in the case where the volume fraction is relatively low (20%) are noticeable but small (between 10 and 20%).

The effect of applied axial stress on the variation of the martensitic volume fraction in SMA particulate composites is illustrated in Figure 6 for an SMA volume fraction equal to 20% and 50%. Predictably, the range of stresses needed for the transformation loop (from austenite to martensite and back to austenite) is larger if the amount of SMA increases. This reflects a higher stiffness of SMA material, even in the martensitic phase, as compared to the stiffness of the epoxy considered in examples. The results

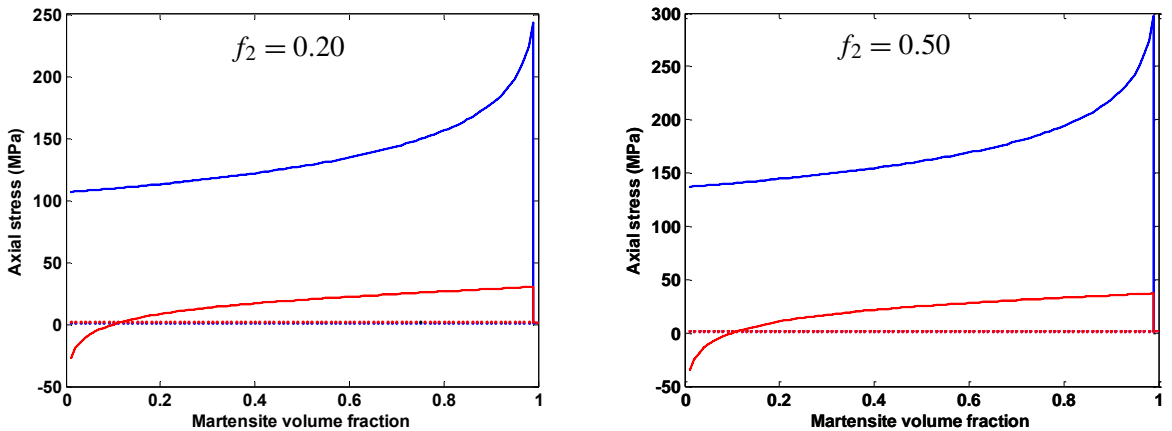


**Figure 6.** Axial stress that has to be applied to a superelastic shape memory alloy particulate composite to cause martensitic (blue curve) or reverse (red curve) transformation. The SMA volume fraction  $f_2$  is 0.20 (left) and 0.50 (right); the temperature is 40 °C.

illustrated in Figures 5 and 6 can further be employed to develop an exact solution for the hysteresis loop of particulate SMA composites (here the word *exact* refers to the solution within the framework of assumptions employed in the theories of Tanaka for SMA and Mori–Tanaka for composite).

## 5. Conclusions

The paper illustrates a two-step approach to the strength and stiffness analyses of fiber-reinforced, particulate-matrix composites. The solution is obtained by a generalization of available micromechanical solutions to three-phase materials. The strength and stiffness of the particulate matrix are specified first, followed with the analysis of the properties of a fiber-reinforced material incorporating the already homogenized matrix.

The numerical analysis shows that adding stiff particles to the matrix results in a significant enhancement of the transverse strength and stiffness, but the benefits are less obvious for the longitudinal strength and stiffness. This reflects a relatively larger contribution of the matrix to the transverse properties of the fiber-reinforced material.

The solution is further extrapolated to composites including shape memory alloy (SMA) inclusions. The exact solution is obtained for the stiffness of such composites, eliminating the need to assume a transformation law (a relationship between the increments of the martensitic fraction and the tensor of the transformation strain) and the associated incremental procedure. As follows from numerical examples, the stiffness of particulate SMA composites is significantly influenced by the stress-induced phase transformation.

### Appendix: Incremental Mori–Tanaka approach to the homogenization of multi-phase materials

Consider a composite material with a relatively high volume fraction of inclusions  $f_i$  ( $i = 2, \dots, N$ ). The procedure utilizes an incremental homogenization that begins with embedding a low volume fraction of inclusions into the matrix, so  $f_1^{(1)} + \sum_{i=2}^N f_i^{(1)} = 1$ , where the superscript identifies the step number.

The stiffness of the material at this first step is evaluated using a counterpart of Equation (19):

$$\mathbf{L}^{(1)} = \mathbf{L}_1 + \sum_{i=2}^N f_i^{(1)} (\mathbf{L}_i - \mathbf{L}_1) \mathbf{T}_i (f_1^{(1)} \mathbf{I} + f_2^{(1)} \mathbf{T}_2 + \dots + f_N^{(1)} \mathbf{T}_N)^{-1}, \quad (\text{A1})$$

where

$$\mathbf{T}_i = [\mathbf{I} + \mathbf{S}_i \mathbf{L}_1^{-1} (\mathbf{L}_i - \mathbf{L}_1)]^{-1}. \quad (\text{A2})$$

The Eshelby tensor at the first step is calculated using the properties of the matrix material.

The incremental procedure at the following steps can easily be developed. For example, at the  $j$ -th step a prescribed increment of inclusions is added to the matrix that already contains inclusions incorporated at the previous steps, so that  $f_1^{(j)} + \sum_{i=2}^N f_i^{(j)} = 1$  and

$$\mathbf{L}^{(j)} = \mathbf{L}^{(j-1)} + \sum_{i=2}^N f_i^{(j)} (\mathbf{L}_i - \mathbf{L}^{(j-1)}) \mathbf{T}_i^{(j)} (f_1^{(j)} \mathbf{I} + f_2^{(j)} \mathbf{T}_2^{(j-1)} + \dots + f_N^{(j)} \mathbf{T}_N^{(j-1)})^{-1} \quad (\text{A3})$$

$$\mathbf{T}_i^j = [\mathbf{I} + \mathbf{S}_i^{(j)} (\mathbf{L}_1^{(j-1)})^{-1} (\mathbf{L}_i - \mathbf{L}^{(j-1)})]^{-1}. \quad (\text{A4})$$

The Eshelby tensor at the  $j$ -th step is calculated using the properties of the material evaluated at the  $(j-1)$ -st step. The properties of inclusions do not change during the procedure, but the tensor of stiffness of the matrix is continuously updated. The suggested procedure enables us to maintain the volume fraction of additional inclusions at each step below the recommended accuracy limit of the Mori–Tanaka approach. Accordingly, at each step,  $\sum_{i=2}^N f_i^{(j)} < r$ , where  $r$  is prescribed (it could be limited to 0.2 or 0.3, depending on the desirable accuracy).

## References

- [Benveniste 1987] Y. Benveniste, “A new approach to the application of Mori–Tanaka’s theory in composite materials”, *Mech. Mater.* **6**:2 (1987), 147–157.
- [Birman 1997] V. Birman, “Review of mechanics of shape memory alloy structures”, *Appl. Mech. Rev. (ASME)* **50** (1997), 629–645.
- [Birman and Byrd 2007] V. Birman and L. W. Byrd, “Modeling and analysis of functionally graded materials and structures”, *Appl. Mech. Rev. (ASME)* **60**:5 (2007), 195–216.
- [Birman et al. 1996] V. Birman, D. A. Saravanos, and D. A. Hopkins, “Micromechanics of composites with shape memory alloy fibers in uniform thermal fields”, *AIAA J.* **34**:9 (1996), 1905–1912.
- [Boyd and Lagoudas 1993] J. G. Boyd and D. C. Lagoudas, “Thermomechanical response of shape memory composites”, *Proc. SPIE* **1917** (1993), 774–790.
- [Cardone et al. 2004] D. Cardone, E. Coelho, M. Dolce, and F. Ponzo, “Experimental behaviour of R/C frames retrofitted with dissipating and re-centering braces”, *J. Earthquake Eng.* **8**:3 (2004), 361–396.
- [Christensen 2007] R. M. Christensen, “A comprehensive theory of yielding and failure for isotropic materials”, *J. Eng. Mater. Technol. (ASME)* **129**:2 (2007), 173–181.
- [Daniel and Ishai 2006] I. M. Daniel and O. Ishai, *Engineering mechanics of composite materials*, 2nd ed., Oxford University Press, New York, 2006.
- [Eshelby 1957] J. D. Eshelby, “The determination of the elastic field of an ellipsoidal inclusion, and related problems”, *Proc. R. Soc. Lond. A* **241**:1226 (1957), 376–396.
- [Genin and Birman 2009] G. M. Genin and V. Birman, “Micromechanics and structural response of functionally graded, particulate-matrix, fiber-reinforced composites”, *Int. J. Solids Struct.* **46**:10 (2009), 2136–2150.
- [Hu and Weng 2000] G. K. Hu and G. J. Weng, “The connections between the double-inclusion model and the Ponte Castaneda–Willis, Mori–Tanaka, and Kuster–Toksoz models”, *Mech. Mater.* **32**:8 (2000), 495–503.
- [Jiang and Batra 2002] B. Jiang and R. C. Batra, “Effective properties of a piezocomposite containing shape memory alloy and inert inclusions”, *Continuum Mech. Therm.* **14**:1 (2002), 87–111.
- [Jonnalagadda et al. 1998] K. D. Jonnalagadda, N. R. Sottos, M. A. Qidwai, and D. C. Lagoudas, “Transformation of embedded shape memory alloy ribbons”, *J. Intell. Mater. Syst. Struct.* **9**:5 (1998), 379–390.
- [Kakavas and Kontoni 2005] P. A. Kakavas and D.-P. N. Kontoni, “Numerical investigation of the stress field of particulate reinforced polymeric composites subjected to tension”, *Int. J. Numer. Methods Eng.* **65**:7 (2005), 1145–1164.
- [Kanaun and Jeulin 2001] S. K. Kanaun and D. Jeulin, “Elastic properties of hybrid composites by the effective field approach”, *J. Mech. Phys. Solids* **49**:10 (2001), 2339–2367.
- [Lagoudas 2008] D. C. Lagoudas (editor), *Shape memory alloys: modeling and engineering applications*, Springer, New York, 2008.
- [Lu and Weng 2000] Z. K. Lu and G. J. Weng, “A two-level micromechanical theory for a shape-memory alloy reinforced composite”, *Int. J. Plast.* **16**:10–11 (2000), 1289–1307.
- [Luo and Weng 1989] H. A. Luo and G. J. Weng, “On Eshelby’s  $S$ -tensor in a three-phase cylindrically concentric solid, and the elastic moduli of fiber-reinforced composites”, *Mech. Mater.* **8**:2–3 (1989), 77–88.
- [McCormick et al. 2006] J. McCormick, R. DesRoches, D. Fugazza, and F. Auricchio, “Seismic vibration control using super-elastic shape memory alloys”, *J. Eng. Mater. Technol. (ASME)* **128**:3 (2006), 294–301.

- [Milton 2002] G. W. Milton, *The theory of composites*, Cambridge Monographs on Applied and Computational Mathematics **6**, Cambridge University Press, Cambridge, 2002.
- [Sato and Tanaka 1988] Y. Sato and K. Tanaka, “Estimation of energy dissipation in alloys due to stress-induced martensitic transformation”, *Res Mech.* **23** (1988), 381–393.
- [Tanaka 1986] K. Tanaka, “A thermomechanical sketch of shape memory effect: one dimensional tensile behavior”, *Res Mech.* **18** (1986), 251–263.
- [Tandon and Weng 1986] G. P. Tandon and G. J. Weng, “Stress distribution in and around spheroidal inclusions and voids at finite concentration”, *J. Appl. Mech. (ASME)* **53** (1986), 511–518.
- [Torquato 2001] S. Torquato, *Random heterogeneous materials: microstructure and macroscopic properties*, Interdisciplinary Applied Mathematics **16**, Springer, New York, 2001.
- [Tucker and Liang 1999] C. L. Tucker, III and E. Liang, “Stiffness predictions for unidirectional short-fiber composites: review and evaluation”, *Compos. Sci. Technol.* **59**:5 (1999), 655–671.
- [Vel and Batra 2004] S. S. Vel and R. C. Batra, “Three-dimensional exact solution for the vibration of functionally graded rectangular plates”, *J. Sound Vib.* **272**:3–5 (2004), 703–730.

Received 16 Dec 2008. Revised 9 Feb 2009. Accepted 12 Feb 2009.

VICTOR BIRMAN: [vbirman@mst.edu](mailto:vbirman@mst.edu)

Engineering Education Center, Missouri University of Science and Technology, One University Boulevard,  
St. Louis, MO 63121, United States